Accepted Manuscript

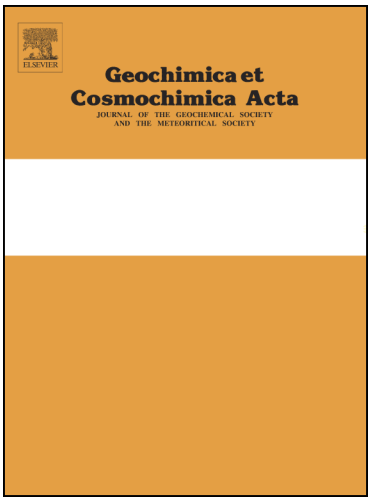

Prediction of Equilibrium Isotopic Fractionation of the Gypsum/Bassanite/Water System using First-Principles Calculations

Tao Liu, Emilio Artacho, Fernando Gázquez, Gregory Walters, David Hodell

PII: S0016-7037(18)30498-8
DOI: https://doi.org/10.1016/j.gca.2018.08.045
Reference: GCA 10918

To appear in: *Geochimica et Cosmochimica Acta*

Received Date: 2 January 2018
Accepted Date: 29 August 2018

Please cite this article as: Liu, T., Artacho, E., Gázquez, F., Walters, G., Hodell, D., Prediction of Equilibrium Isotopic Fractionation of the Gypsum/Bassanite/Water System using First-Principles Calculations, *Geochimica et Cosmochimica Acta* (2018), doi: https://doi.org/10.1016/j.gca.2018.08.045

Prediction of Equilibrium Isotopic Fractionation of the Gypsum/Bassanite/Water System using First-Principles Calculations

Tao Liu[a,b,*], Emilio Artacho[b], Fernando Gázquez[a,c], Gregory Walters[a], David Hodell[a]

[a] Godwin Laboratory for Palaeoclimate Research, Department of Earth Sciences, University of Cambridge, Downing Street, Cambridge CB2 3EQ, United Kingdom

[b] Theory of Condensed Matter, Cavendish Laboratory, University of Cambridge, J. J. Thomson Ave, Cambridge CB3 0HE, United Kingdom

[c] School of Earth and Environmental Sciences. University of St. Andrews. St Andrews, KY16 9AL, Scotland, United Kingdom.

* Corresponding author. E-mail address: tl439@cam.ac.uk (T. Liu).

Abstract

The stable isotopes ($^{18}O/^{16}O$, $^{17}O/^{16}O$ and $^{2}H/^{1}H$) of structurally-bound water (also called hydration water) in gypsum ($CaSO_4 \cdot 2H_2O$) and bassanite ($CaSO_4 \cdot 0.5H_2O$) can be used to reconstruct the isotopic composition of paleo-waters. Understanding the variability of the isotope fractionation factors between the solution and the solid ($\alpha^{17}O_{mineral\text{-}water}$, $\alpha^{18}O_{mineral\text{-}water}$ and $\alpha D_{mineral\text{-}water}$) is crucial for applying this proxy to paleoclimatic research. Here we predict the theoretical equilibrium fractionation factors for triple oxygen and hydrogen isotopes in the gypsum-water and bassanite-water systems between 0 °C and 60 °C. We apply first-principles using density functional theory within the harmonic approximation. Our theoretical results for $\alpha^{18}O_{gypsum\text{-}water}$ (1.00347±0.00037) are in agreement with previous experimental studies, whereas $\alpha D_{gypsum\text{-}water}$ agrees only at temperatures above 25 °C. At lower temperatures, the experimental values of $\alpha D_{gypsum\text{-}water}$ are consistently higher than theoretical values (e.g. 0.9749 and 0.9782, respectively, at 3 °C), which can be explained by kinetic effects that affect gypsum precipitation under laboratory conditions at low temperature. We predict that $\alpha^{18}O_{bassanite\text{-}water}$ is similar to $\alpha^{18}O_{gypsum\text{-}water}$ in the temperature range of 0 °C to 60 °C. Both $\alpha^{18}O_{gypsum\text{-}water}$ and $\alpha^{18}O_{bassanite\text{-}water}$ show a small temperature dependence of ~0.0000122 per °C, which is negligible for most paleoclimate studies. The theoretical relationship between $\alpha^{17}O_{gypsum\text{-}water}$ and $\alpha^{18}O_{gypsum\text{-}water}$ ($\theta = \frac{\ln\alpha^{17}O}{\ln\alpha^{18}O}$) from 0 °C to 60 °C is 0.5274±0.00063. The relationship is very insensitive to temperature (0.00002 per °C). The fact that $\delta^{18}O$ values of gypsum hydration water are greater than free water ($\alpha^{18}O_{gypsum\text{-}water} > 1$) whereas δD values of gypsum hydration water are less than free water ($\alpha D_{gypsum\text{-}water} < 1$) is explained by phonon theory. We conclude that calculations from first-principles using density functional theory within the harmonic approximation can accurately predict fractionation

factors between structurally-bound water of minerals and free water.

Keywords: Gypsum, Bassanite, Fractionation factor, First-principles

1. Introduction

Gyspum ($CaSO_4•2H_2O$) is a common hydrous mineral on Earth and has also been shown to be abundant on Mars (Showstack, 2011). The hemihydrate form of calcium sulfate, bassanite ($CaSO_4•0.5H_2O$), is a precursor to gypsum formation (Wang and Meldrum, 2012; Van Driessche et al., 2012), but is rarely found in natural mineral deposits on Earth and more often occurs as a mixture of gypsum and/or anhydrite ($CaSO_4$). Nevertheless, the presence of bassanite, together with gypsum and other hydrous minerals on Mars (Wray et al., 2010), has generated considerable interest in how these minerals form and their paleoenvironmental significance.

The oxygen (^{16}O, ^{17}O and ^{18}O) and hydrogen (^{1}H and ^{2}H (D)) isotopes of structurally-bound water in minerals, also known as hydration water, provide a rich source of information on the environmental conditions at the time of mineral formation (Hodell et al., 2012; Evans et al., 2015; Grauel et al., 2016; Gázquez et al., 2017b; Gázquez et al., 2017a; Herwartz et al., 2017; Gázquez et al., 2018). Indeed, under certain conditions, the isotopic composition of hydration water in some minerals (e.g. gypsum) record the isotope values of the mother water with an offset between the free solution and mineral hydration water because of isotope fractionation (Gonfiantini and Fontes, 1963; Sofer, 1978; Hodell et al., 2012; Tan et al., 2014; Gázquez et al., 2017b; Herwartz et al., 2017). The fractionation factor ($\alpha_{mineral\text{-}water}$) can be expressed as:

$$\alpha_{mineral-water} = \frac{R_{mineral}}{R_{water}}$$

where R is the ratio of the heavy to light isotope (e.g., $^{18}O/^{16}O$, $^{17}O/^{16}O$, D/H) of the mineral hydration water and mother water, respectively. The fractionation factor can also be expressed in terms of the δ-values of the two species (e.g., hydration and mother water):

$$\alpha_{mineral-water} = \frac{\delta_{mineral} + 1000}{\delta_{water} + 1000}$$

where $\delta_{mineral}$ and δ_{water} denote the isotopic ratio of the mineral and the mother water relative to the international standard V-SMOW (Vienna-Standard Mean Ocean Water). Under certain conditions, the fraction factor can be approximated by the isotopic difference between the mineral and water (ε):

$$\varepsilon = 1000 \ln \alpha \approx \delta_{mineral} - \delta_{water}$$

Applying the isotopic composition of mineral hydration water as a paleoclimatic proxy requires detailed knowledge of these fractionation factors and their dependence on environmental parameters, such as temperature and salinity (Gázquez et al., 2017b). The first experimental measurements of the fractionation factors for $^{18}O/^{16}O$ and D/H in the gypsum-water system were performed by Gonfiantini and Fontes (1963) and Fontes and Gonfiantini (1967), who reported values of 1.004 and 0.98 for $\alpha^{18}O_{gypsum\text{-}water}$ and $\alpha D_{gypsum\text{-}water}$, respectively. These values agree with the results of more recent studies within analytical uncertainties (Matsuyaba and Sakai, 1973; Sofer, 1978; Hodell et al., 2012). The $\alpha^{18}O_{gypsum\text{-}water}$ was reported to be insensitive to temperature between 12 °C and 57 °C (Gonfiantini and Fontes, 1963). Hodell et al. (2012) confirmed the temperature-insensitivity of $\alpha^{18}O_{gypsum\text{-}water}$; however, they found a small positive temperature dependence (0.00012 per °C) for $\alpha D_{gypsum\text{-}water}$ between 12 °C and 37 °C. More recently, Gázquez et al. (2017b) empirically measured $\alpha^{18}O_{gypsum\text{-}water}$ and $\alpha D_{gypsum\text{-}water}$ more precisely to be 1.0035±0.0002 and 0.9805±0.0035 between 3 °C and 55 °C, respectively. The $\alpha^{18}O_{gypsum\text{-}water}$ was found to decrease by 0.00001 per °C in this temperature range, whereas $\alpha D_{gypsum\text{-}water}$ increases by 0.0001 per °C. These authors concluded that in the temperature range under which gypsum forms in most natural environments (e.g. 10-30 °C), the dependence of the isotope fractionation factors with temperature is insignificant. However, temperature must be taken into account when applying fractionation factors to hydrothermal or cryogenic gypsum, especially for $\alpha D_{gypsum\text{-}water}$. Importantly, the $\alpha^{18}O_{gypsum\text{-}water}$ and $\alpha D_{gypsum\text{-}water}$ at or less than 0 °C is still unknown because experimental limitations prevent the precipitation of gypsum at temperatures close to the freezing point of water.

Salinity has been also found to affect $\alpha^{18}O_{gypsum\text{-}water}$ when salt concentration exceeds 150 g/l of NaCl, with no significant effect at lower concentrations (Gázquez et al., 2017b). The salt effect on $\alpha D_{gypsum\text{-}water}$ is relevant even at relatively low salinities (e.g. 80 g/l of NaCl), so salt corrections are needed when dealing with gypsum formed from brines (e.g. Dead Sea, purely evaporated seawater gypsum, etc.; see Section 5.4.4 for discussion of salt corrections). However, many gypsum deposits do not necessarily form from brines *per se*, but rather from low-salinity waters. For example, the salinity of water rarely exceeds 5 g/l in many gypsum-precipitating lakes (Hodell et al., 2012; Gázquez et al., 2018). Additionally, relatively low salt concentrations have been found in fluid inclusions of hydrothermal gypsum (Garofalo et al., 2010) and in fluid inclusions of gypsum deposits formed in marine environments affected by freshwater (Natalicchio et al., 2014; Evans et al., 2015).

To our knowledge there is no reported value for $\alpha^{18}O$ and αD for the bassanite-water system, mainly because of the difficulty in synthesizing pure bassanite (Wang and Meldrum, 2012; Van Driessche et al., 2012). Bassanite can be synthesized but isotope measurements of its hydration water and the original solution are made difficult by isotope exchange with reagents used for bassanite stabilization (i.e. alcohols) (Tritschler

et al., 2015a; Tritschler et al., 2015b). Thus, prediction of bassanite-water fractionation from first-principles offers a promising solution.

In addition to the routine measurement of $^{18}O/^{16}O$ and $^{2}H/^{1}H$ in natural waters and mineral hydration water, recent analytical developments permit the precise measurement of triple oxygen isotopes ($^{16}O/^{17}O/^{18}O$) and the derived parameter ^{17}O-excess (also called $\Delta^{17}O$) (Barkan and Luz, 2005; Luz and Barkan, 2010; Steig et al., 2014). This parameter can be defined as:

$$^{17}\text{O-excess} = \ln(\delta^{17}O + 1) - 0.528 \ln(\delta^{18}O + 1)$$

where $\delta^{17}O$ and $\delta^{18}O$ denote the $^{17}O/^{16}O$ and $^{18}O/^{16}O$ in water standardized to the VSMOW-SLAP scale (Barkan and Luz, 2005; Luz and Barkan, 2010; Schoenemann et al., 2013). The value of 0.528 has been proposed to describe the $\delta^{17}O$ and $\delta^{18}O$ relationship in rainwater worldwide.

During evaporation of water, each isotope ratio (i.e. $^{18}O/^{16}O$, $^{17}O/^{16}O$ and $^{2}H/^{1}H$) follows a slightly different fractionation, leading to variability in ^{17}O-excess and d-excess (Gázquez et al., 2017b; Herwartz et al., 2017). The d-excess is relatively sensitive to temperature and relative humidity, whereas the $\theta_{\text{vapor-liquid}}$ value ($\frac{\ln\alpha^{17}O}{\ln\alpha^{18}O}$) of the evaporation process is largely insensitive to temperature, but highly dependent on relative humidity. This means that ^{17}O-excess can potentially be used for quantitative paleo-humidity reconstructions, as demonstrated using lacustrine gypsum deposits (Gázquez et al., 2018). Given the large differences in $\Delta^{17}O$ between Mars and Earth (Franchi et al., 1999), triple oxygen isotope analysis is also useful in determining whether gypsum/bassanite hydration water in Martian meteorites preserves its primary signal or is modified by mixing/exchange with terrestrial water (Greenwood et al., 2009). In addition, the triple oxygen isotope composition of Martian gypsum/bassanite deposits (Showstack, 2011; Massé et al., 2012) would provide information about the hydrological processes that occurred during wetter stages of Mars' history.

The ^{17}O-excess variability in natural waters on Earth (including evaporated waters) varies by less than 150 per meg (0.15 ‰) (Luz and Barkan, 2010; Herwartz et al., 2017; Gázquez et al., 2018) relative to an analytical precision for ^{17}O-excess that is better than 10 per meg (1SD; (Luz and Barkan, 2010; Gázquez et al., 2015)). Inaccuracy in the $\theta_{\text{gypsum-water}}$ value can lead to significant errors when reconstructing the ^{17}O-excess of paleo-waters from gypsum hydration water. For example, a variation of 0.005 units in $\theta_{\text{gypsum-water}}$ produces a bias of 15 per meg in the reconstructed ^{17}O-excess. Such a difference might lead to different interpretations when modelling and comparing ^{17}O-excess values of paleo- and modern waters. Consequently, accurate determination of the $\theta_{\text{gypsum-water}}$ value is crucial for using triple oxygen isotopes to reconstruct past hydrological conditions.

Gázquez et al. (2017b) measured a $\theta_{gypsum\text{-}water}$ value of 0.5297±0.0012 and concluded that this parameter is insensitive to temperature between 3 °C and 55 °C. This measured value is close to the greatest theoretical value of θ in any mass-dependent fractionation process of the triple oxygen isotope system, which ranges from 0.5200 to 0.5305 (Matsuhisa et al., 1978; Cao and Liu, 2011; Bao et al., 2016). Herwartz et al. (2017) reported a slightly lower $\theta_{gypsum\text{-}water}$ value of 0.5272±0.0019.

Theoretical studies of isotopic fractionation are particularly useful in systems that are difficult to characterize experimentally, or when empirical data are rare or absent (Richet et al., 1977; Méheut et al., 2007; Qin et al., 2016). Theoretical calculations can extend the temperature range over which fractionation factors can be used, which is especially relevant for low-temperature mineral-solution fractionation where isotopic equilibrium takes a long time to achieve. Theory also offers insights into the causes of isotopic fractionation, such as changing properties of vibration and chemical bonding. Theoretical calculations of high accuracy have been made for molecules in the gas phase (Richet et al., 1977). First-principles calculations have also been used for solid materials within the framework of density functional theory (DFT), including minerals such as quartz, kaolinite, brucite, talc, gibbsite, albite and garnet. (Méheut et al., 2007; Reynard and Caracas, 2009; Méheut and Schauble, 2014; Qin et al., 2016). Here we use DFT to determine the equilibrium $\alpha^{17}O_{mineral\text{-}water}$, $\alpha^{18}O_{mineral\text{-}water}$ and $\alpha D_{mineral\text{-}water}$ values for the gypsum-water and bassanite-water systems. We compare the theoretical calculations with published experimental results for gypsum-water. Building upon successful convergence of empirical and theoretical results for gypsum, we determine for the first time the bassanite-water fractionation factors for triple oxygen and hydrogen isotopes, and predict the theoretical dependence of these parameters with temperature. Lastly, we seek to understand the origin of the opposite direction of the fractionation factors for δD (<1) and $\delta^{18}O$ (>1) in many hydrous minerals by using gypsum as a case study.

2. Method to calculate fractionation factors

The isotopic fractionation factors of gypsum-water and bassanite-water are calculated by combining the theoretical mineral-vapor fractionation factors and the experimental water-vapor fractionation factors (Horita and Wesolowski, 1994; Barkan and Luz, 2005) as follows (Méheut et al., 2007):

$$\alpha^{18}O_{mineral\text{-}water} = \frac{\alpha^{18}O_{mineral-vapor}}{\alpha^{18}O_{water-vapor}} \quad (1)$$

$$\alpha D_{mineral\text{-}water} = \frac{\alpha D_{mineral-vapor}}{\alpha D_{water-vapor}} \quad (2)$$

Because the reported theoretical results depend on the experimental fractionation values $\alpha^{18}O_{water\text{-}vapor}$, the errors of $\alpha^{18}O_{water\text{-}vapor}$ (±0.00002 ~ 0.00006) should be propagated to the theoretical results (Horita and Wesolowski, 1994; Barkan and Luz, 2005).

The isotopic fractionation factor between two phases can be calculated as (Richet et al., 1977; Méheut et al., 2007):

$$\alpha_{\text{mineral-vapor}} = \frac{\beta_{\text{mineral}}}{\beta_{vapor}} \quad (3)$$

where β_{mineral} and β_{vapor} are the reduced fractionation factors for mineral and vapor, which in the dilute limit are:

$$\beta = \frac{1}{n}\sum_{i=1}^{n}\left[\frac{Q(AY_{n-1}Y_i^*)}{Q(AY_n)}\right]\left[\frac{m_Y}{m_{Y*}}\right]^{3/2} \quad (4)$$

Q is the partition function, Y is the oxygen (or hydrogen) in the hydration water of gypsum and bassanite, n is the number of oxygen (or hydrogen) atoms in the hydration water, A is all the other atoms except oxygen (or hydrogen) in hydration water. $Q(AY_{n-1}Y_i^*)$ is the partition function of the mineral with one Y replaced by Y* (Y is the light isotope, Y* is the heavy isotope), $Q(AY_n)$ is the partition function of the mineral with no Y* replacement, m_Y is the atom mass of Y, m_{Y*} is the atom mass of Y*. The diluted limit is obtained by substituting one heavy isotope in a large sample of the light isotope minerals or liquid. If several different substitutions are possible, fractionation factors are calculated for all substitutions separately, and then averaged as in e.q. 4.

We calculate the vibrational frequencies for a water molecule, gypsum and bassanite within the harmonic approximation. Water vapor is simulated by using an isolated H_2O molecule in a 20x20x20 $Å^3$ box with periodic boundary conditions. The partition function of the water molecule is composed of translational, rotational and vibrational contributions. The details of the methods used for calculating the translational and rotational contributions were described by Méheut et al. (2007).

The harmonic vibrational partition function for the molecule is calculated as follows:

$$Q_{vib} = \prod_i^{modes} \frac{e^{-\frac{\hbar\omega_i}{2kT}}}{1-e^{-\frac{\hbar\omega_i}{kT}}} \quad (5)$$

i runs over the three vibrational modes of an isolated water molecule.

For a solid phase, the partition function has only vibrational contributions,

$$Q = Q_{vib} = \left(\prod_i^{bands}\prod_{\vec{q}}^{N_q}\frac{e^{-\frac{\hbar\omega_i(\vec{q})}{2kT}}}{1-e^{-\frac{\hbar\omega_i(\vec{q})}{kT}}}\right)^{1/N_q} \quad (6)$$

where i now runs over bands, and $\vec{q}$ runs over the N_q points in the sampling of the Brillouin zone in reciprocal space.

3. Computational details

We carried out first-principles calculations based on density functional theory (DFT) using the Siesta computer program with numerical atomic orbital basis sets (Soler et al., 2002). All calculations were done with the generalized gradient approximations (GGA), using the Perdew-Burke-Ernzerhof scheme for solids (PBEsol) (Perdew et al., 2008) functional for electronic exchange and correlation. Other functionals, such as PBE (Perdew et al., 1996) and LDA (Perdew and Zunger, 1981), were also tested to determine functional dependence and find the functional that gives the structural and vibrational values closest to experimental data. The LO-TO splitting effect was also included in the vibrational calculations (Gonze and Lee, 1997). Core electrons were replaced by *ab initio* norm conserving pseudopotentials, generated using the Troullier-Martins scheme (Troullier and Martins, 1991a; Troullier and Martins, 1991b). Because of the significant overlap between the 3*p* semi-core states and valence states, the 3*p* electrons of Ca were considered as valence electrons and explicitly included in the simulations. The Ca, S, O, and H pseudopotentials were generated using the ATOM software (Soler et al., 2002) and tested thoroughly. The basis set functions for all the elements were also generated using diatomic models (Oroya et al., 2016). The basis set and pseudopotential for Ca were thoroughly tested for CaO vibrations including LO-TO splitting. A plane-wave energy cutoff of 600 Ry for the real-space integration grid, and a **k**-grid cutoff of 10 Å for the Brillouin zone sampling were used for the gypsum (48 atoms) and bassanite (90 atoms) unit cells, as found in convergence tests. Structural relaxations were carried out by minimizing the total energy until the smallest force component absolute value was under 0.001 eV/ Å, and the smallest stress component under 0.01 GPa. The tolerance of density matrix element change for self-consistency was 10^{-5}. Supercells of 3x1x3 (gypsum) and 1x3x1 (bassanite) were used to calculate the force constants by finite displacements, to get the full phonon dispersion from finite differences. For the phonons, the Brillouin zone was sampled with 220 points for gypsum and 290 points for bassanite. The starting structures for relaxation of gypsum and bassanite were obtained from single-crystal X-ray results (Bezou et al., 1991; Schofield et al., 1996).

4. Results

4.1. Relaxed structures

The structures of gypsum, bassanite, and the water molecule were relaxed using DFT. Our results for the water molecule agree well with experimental data, with 1% greater value for the OH bond length, and a 0.03% smaller value for H-O-H angle as compared to experimental values (Császár et al., 2005). The optimized structures of gypsum and bassanite are shown in Fig. 1. Gypsum has a monoclinic structure, whereas bassanite has an orthorhombic structure. The lattice parameters of the optimized structure of gypsum are 6.461 Å, 14.979 Å, 5.661 Å; for bassanite they are 12.023 Å, 6.917 Å, 12.611 Å. These lattice parameters are all in agreement with neutron powder diffraction results

(Bezou et al., 1991; Schofield et al., 1996), being within 0.9% of the experimental values (Table 1).

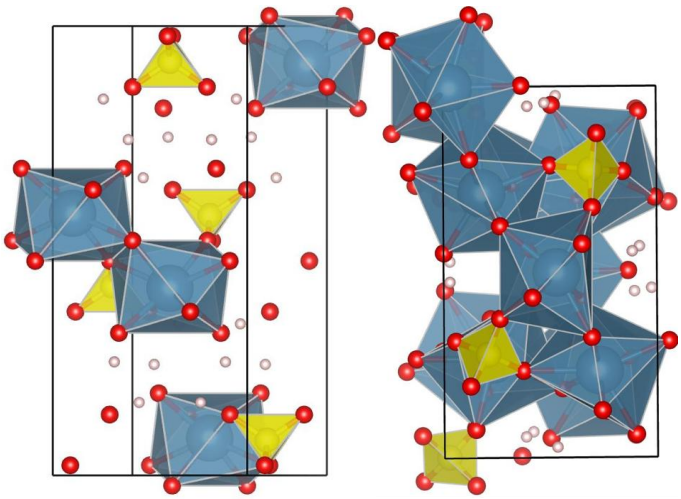

(a) (b)

Fig. 1. Structure of gypsum (a) and bassanite (b) with oxygen in red, hydrogen in white, calcium in green center, sulfur in yellow center. The structure is optimized using density function theory starting from experimental crystal data (Bezou et al., 1991; Schofield et al., 1996) . The figure was produced using VESTA (Momma and Izumi, 2011).

Table 1. The optimized lattice parameters for gypsum and bassanite, compared with experimental results. Diff stands for the difference percentage between theoretical and experimental results.

Lattice	PBEsol	Expt.[a]	diff %	PBEsol	Expt.[b]	diff %
	gypsum			bassanite		
a	6.460	6.491	-0.48	12.023	12.019	0.03
b	14.979	15.105	-0.83	6.916	6.930	0.20
c	5.661	5.674	-0.23	12.611	12.670	0.47

[a] (Schofield et al., 1996), [b] (Bezou et al., 1991)

4.2. Vibrational frequencies

Vibrational frequencies are needed to calculate the reduced fractionation factor β and eventually the fractionation factor α. Although they are all consistent with the experimental IR and Raman spectra (Prieto-Taboada et al., 2014), the values obtained from PBEsol are significantly closer to the ones obtained from experimental infrared and Raman spectra than those obtained from PBE (optimized structure obtained by PBEsol is closer to the experimental results than that obtained by PBE). It is quite common to scale all frequencies with an empirical single scale factor to obtain a better match of the experimental spectra. However, the β and α fractionation coefficients in this paper were

calculated solely from the raw theoretical harmonic frequencies obtained from DFT, as the better accuracy of PBEsol renders the scale factor unnecessary.

Our calculated gamma phonons of gypsum are in agreement with the experimental values (Prieto-Taboada et al., 2014), with O-H symmetric and asymmetric stretching at 3300 - 3500 cm^{-1}, scissor bending at 1600 cm^{-1} and S-O stretching of the SO_4^{2-} group at 1000 cm^{-1}. Our results also show that the O-H stretching of bassanite as red-shifted (by 60-70 cm^{-1}) compared to that of gypsum in agreement with the experimentally measured shift (60 cm^{-1}) (Prieto-Taboada et al., 2014).

4.3. Isotopic fractionation factor

4.3.1. Oxygen isotope fractionation factor for the gypsum-water system

We compare the theoretical $\alpha^{18}O_{gypsum\text{-}water}$ (expressed as 1000 $ln\alpha^{18}O_{gypsum\text{-}water}$) with experimental results (Gázquez et al., 2017b) over the temperature range from 0°C to 60°C (Fig. 2a). Our theoretical results agree with the experimental fractionation factors with a maximum difference of only 0.0004. The LO-TO splitting is not included in the fractionation calculation because even when testing for the gamma phonon only, which is an overestimate of the real effect, there is only a 0.00002 difference for $\alpha^{18}O_{gypsum\text{-}water}$ caused by LO-TO splitting, which is negligible. The dependence of $\alpha^{18}O_{gypsum\text{-}water}$ with temperature is well described by a third order polynomial (fitting parameters for α and β are listed in Table 2), whereas the experimental data were fit by a linear equation because of the analytical errors associated with the measurements (Gázquez et al., 2017b). The temperature dependence of $\alpha^{18}O_{gypsum\text{-}water}$ is about -0.0000122 per °C.

The $\alpha^{17}O_{gypsum\text{-}water}$ overlaps with experimental results, with maximum differences of 0.000098 (Fig. 2(b)) (Gázquez et al., 2017b). Our theoretical result of $\theta_{gypsum\text{-}water}$ (0.5275 at 30 °C) is 0.001-0.002 less than the value of 0.5297±0.0012 reported by Gázquez et al. (2017b), but in good agreement with the value of 0.5272±0.0019 reported by Herwartz et al. (2017) (Fig2(c)). Our results show that $\theta_{gypsum\text{-}water}$ are well described using a third order polynomial with a weaker temperature dependence (0.00002 per °C) than the individual fractionation factors (Table 2). This is because $\alpha^{18}O_{gypsum\text{-}water}$ and $\alpha^{17}O_{gypsum\text{-}water}$ change in a very similar fashion as a function of temperature, because of mass-dependent isotope fractionation.

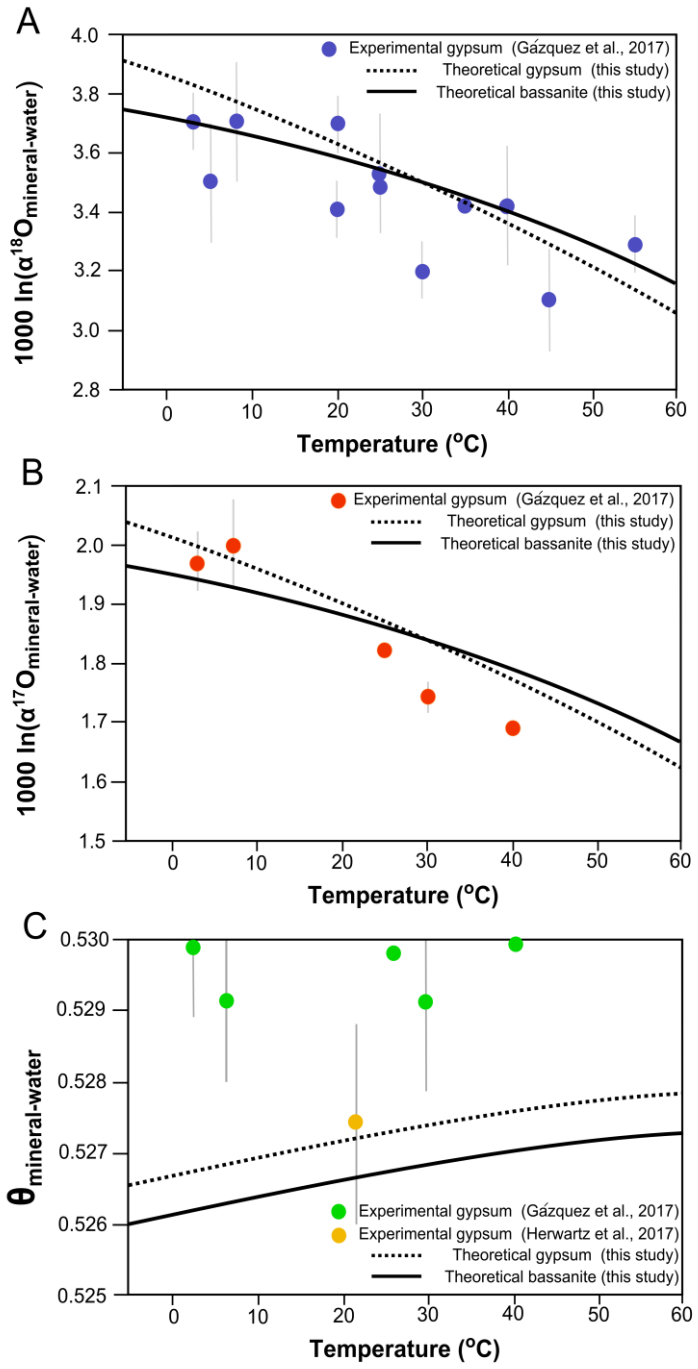

Fig. 2. 1000 lnα^{18}O (‰) (a), 1000 lnα^{17}O (‰) (b) and θ (c) of gypsum-water (dotted lines) and bassanite-water (solid lines) as a function of temperature, together with the experimental results of 1000 lnα^{18}O of gypsum-water (blue dots with error bar (Gázquez et al., 2017b)) (a), 1000 lnα^{17}O of gypsum-water (red dots with error bar (Gázquez et al., 2017b)) (b), and θ of gypsum-water (green dots with error bar (Gázquez et al., 2017b), yellow dots with error bar (Herwartz et al., 2017)) (c). The data for temperature range of 0 to -5 °C is also shown in the plots by extrapolation.

Table 2. Fitting parameters of 1000 lnα (‰) and 1000 lnβ (‰) by third order polynomial aT^3+bT^2+cT+d

in the temperature range of 0 °C to 60 °C.

1000 lnα (‰)	phases	a	b	c	d
$^{18}O/^{16}O$	gypsum-water	$9.0*10^{-7}$	$-1.0*10^{-4}$	$-8.6*10^{-3}$	3.8175
	bassanite-water	$1.0*10^{-6}$	$-1.0*10^{-4}$	$-3.5*10^{-3}$	3.6894
$^{17}O/^{16}O$	gypsum-water	$5.0*10^{-7}$	$-6.0*10^{-5}$	$-4.4*10^{-3}$	2.011
	bassanite-water	$5.0*10^{-7}$	$-8.0*10^{-5}$	$-1.7*10^{-3}$	1.9413
D/H	gypsum-water	$2.0*10^{-3}$	$-4.1*10^{-3}$	$3.380*10^{-1}$	-26.294
	bassanite-water	$2.0*10^{-3}$	$-5.3*10^{-3}$	$5.973*10^{-1}$	-47.582
θ	gypsum-water	$1.0*10^{-9}$	$-3.0*10^{-7}$	$3.0*10^{-5}$	0.5268
	bassanite-water	$2.0*10^{-9}$	$-3.0*10^{-7}$	$4.0*10^{-5}$	0.5262
1000 lnβ (‰)	phases	a	b	c	d
$^{18}O/^{16}O$	gypsum	$-4.0*10^{-6}$	$1.60*10^{-3}$	$-4.085*10^{-1}$	83.294
	bassanite	$-4.0*10^{-6}$	$1.60*10^{-3}$	$-4.034*10^{-1}$	83.165
	vapor	$-5.0*10^{-5}$	$3.90*10^{-3}$	$-1.896*10^{-1}$	67.532
$^{17}O/^{16}O$	gypsum	$-2.0*10^{-6}$	$9.00*10^{-4}$	$-2.162*10^{-1}$	44.12
	bassanite	$-2.0*10^{-6}$	$8.00*10^{-4}$	$-2.135*10^{-1}$	44.05
	vapor	$-1.0*10^{-6}$	$5.00*10^{-4}$	$-1.511*10^{-1}$	35.885
D/H	gypsum	$-1.0*10^{-4}$	$4.71*10^{-2}$	$1.2757*10^{-1}$	2788
	bassanite	$-1.0*10^{-4}$	$4.60*10^{-2}$	$1.2498*10^{-1}$	2766.7
	vapor	$-1.0*10^{-4}$	$4.11*10^{-2}$	$1.1656*10^{-1}$	2708.1

4.3.2. Oxygen isotope fractionation factor for the bassanite-water system

Over the temperature range from 0 to 60 °C, the mean $\alpha^{18}O_{bassanite\text{-}water}$ is 1.00346±0.00018, almost same as the $\alpha^{18}O_{gypsum\text{-}water}$ (1.00347±0.0004) (Fig. 2(a)). The temperature dependence is -0.000009 per °C, similar to $\alpha^{18}O_{gypsum\text{-}water}$. We found that $\alpha^{18}O_{gypsum\text{-}water}$ and $\alpha^{18}O_{bassanite\text{-}water}$ are the same at ~30 °C (1.0035), whereas $\alpha^{18}O_{gypsum\text{-}water} > \alpha^{18}O_{basssanite\text{-}water}$ at lower temperatures and $\alpha^{18}O_{gypsum\text{-}water} < \alpha^{18}O_{basssanite\text{-}water}$ at higher temperatures, with differences not exceeding 0.00013 (Fig. 2a).

4.3.3. Hydrogen isotopes fractionation for the gypsum-water and bassanite-water systems

In general, our predicted $\alpha D_{gypsum\text{-}water}$ values agree well with experimental results (Fig. 3). Note that our theoretical results are extrapolated to cover the temperature range as low as -5 °C). At low temperatures (0 °C and 3 °C), our theoretical $\alpha D_{gypsum\text{-}water}$ is 0.9740 and 0.9748, respectively, with a deviation of about -0.004 from the experimental result of 0.978 at 3 °C. At temperatures greater than 25 °C, our theoretical results agree well with experimental data, with a difference of less than -0.001. For hydrogen isotopes, Gázquez et al. (2017b) suggested that the measured experimental value for $\alpha D_{gypsum\text{-}water}$ could be higher than the actual equilibrium value because of kinetic effects during gypsum precipitation. In contrast, our theoretical results for oxygen isotopes agree with their experimental values on $\alpha^{18}O$, suggesting that kinetic effects are small for $\alpha^{18}O$.

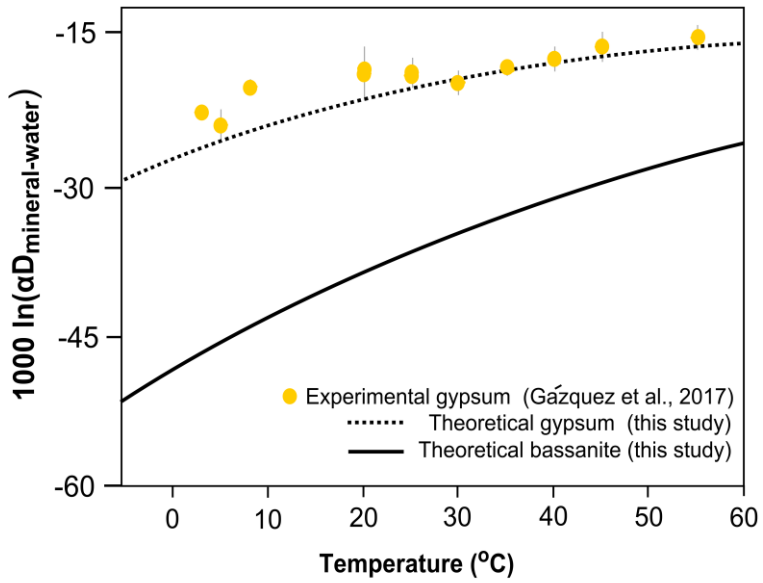

Fig. 3. 1000 lnαD (‰) of gypsum-water (dotted line) and bassanite-water (solid line) as a function of temperature together with the experimental results (yellow dots with error bar) (Gázquez et al., 2017b). Note the much stronger temperature dependence for bassanite than gypsum. The data for the temperature range of 0 to -5 °C is also shown in the plot by extrapolation.

5. Discussion

5.1. Equilibrium isotopic fractionation of $^{18}O/^{16}O$

Our results show that $\alpha^{18}O_{gypsum\text{-}water}$ and $\alpha^{18}O_{basssanite\text{-}water}$ are very similar in the temperature range of 0 to 60 °C, with differences of less than 0.0002. This is because the vibrational frequencies of bassanite and gypsum respond similarly to the replacement of ^{16}O with ^{18}O. Consequently, the partition function and reduced fractionation factors are similar. The average $O(H_2O) - Ca(CaSO_4)$ bond lengths of bassanite (2.332067 Å) and gypsum (2.332075 Å) are almost the same. It is well known that shorter bond lengths correlate with stronger and stiffer bonds and, as a result, the value of β will be greater (Schauble, 2004; Oi Takao et al., 2014). In the case of gypsum and bassanite, very similar bond strengths lead to very similar β values. The temperature effect on $\alpha^{18}O_{gypsum\text{-}water}$ is relatively small, with a variation of less than -0.0000122 per °C, which agrees with the experimental slope of -0.0000116 per °C (Gázquez et al., 2017b). For $\alpha^{18}O_{basssanite\text{-}water}$, the temperature dependence is even smaller (-0.0000087 per °C). A similar temperature effect has been found for $\alpha^{17}O_{gypsum\text{-}water}$ and $\alpha^{17}O_{basssanite\text{-}water}$. Our results demonstrate that the $\alpha^{18}O$ and $\alpha^{17}O$ for gypsum-water and bassanite-water are barely affected by temperature in the range relevant for most paleoclimatic studies (Hodell et al., 2012; Grauel et al., 2016; Gázquez et al., 2018). This lack of temperature dependence provides a distinct advantage when using hydration water to estimate the isotopic composition of

the mother water from which the gypsum or bassanite precipitated.

To extend our understanding of isotopic fractionation to any site in the gypsum structure, we studied the $\alpha^{18}O$ of potential isotope exchange between the ^{18}O atoms in tetrahedral SO_4^{2-} and mother water. This oxygen exchange is difficult to determine experimentally because of the extremely slow kinetic rates of oxygen isotope exchange in SO_4^{2-}, even in solution (Zeebe, 2010). SO_4^{2-} groups are very stable and the energy barrier for exchanging ^{16}O with ^{18}O is much greater than that for any presumed isotope exchange between hydration water and environmental water. Our simulation suggests that $\alpha^{18}O_{SO_4^{2-}-water}$ is 1.023 at 0°C, and decreases to 1.018 at 25 °C and 1.013 at 60 °C, which agrees with the theoretical value of 1.023 at 25 °C obtained by Zeebe (2010). We suggest that the difference of 0.005 between our results and the results obtained by Zeebe (2010) is caused by the different SO_4^{2-} group environments. The oxygen atoms in the SO_4^{2-} groups in our calculations are shared with Ca cation groups, whereas the model considered by Zeebe (2010) dealt with SO_4^{2-} groups in solution surrounded by H_2O molecules. Our results imply that ^{18}O will be more enriched in the tetrahedral SO_4^{2-} structures than in the hydration water, if the exchange process can overcome high-energy barriers towards full equilibrium. However, no evidence of such a process has been observed in natural gypsum deposits from lakes (Hodell et al., 2012; Herwartz et al., 2017; Gázquez et al., 2018), caves (Gázquez et al., 2017b), hydrothermal systems (Chen et al., 2016; Gázquez et al., 2017b) or Messinian marine gypsum (Evans et al., 2015).

5.2. Equilibrium isotopic fractionation factor of D/H

The $\alpha D_{gypsum\text{-}water}$ shows that our theoretical results agree with experimental values (Fig. 3), with a maximum deviation of ~0.004 at low temperatures, which decreases above room temperature. This confirms the results reported by Gázquez et al. (2017a), who found $\alpha D_{gypsum\text{-}water}$ is relatively sensitive to temperature between 3 and 55 °C. However, in the temperature range of many paleoclimatic studies (e.g. 10 to 30 °C) the variation in $\alpha D_{gypsum\text{-}water}$ is only 0.002, leading to small differences of 2‰ when calculating δD values of the mother water.

The temperature dependence of $\alpha D_{bassanite\text{-}water}$ (0.00035 per °C) in the range of 0°C to 60 °C, however, is much steeper than for gypsum-water (more than twice as steep, 0.00016 per °C). The temperature effect is greater at low temperature than at high temperature, indicating that the formation temperature of bassanite needs to be known in order to calculate accurate mother water δD values from the hydration water of bassanite.

5.3. Salinity effects on $\alpha^{18}O_{gypsum\text{-}water}$ and $\alpha D_{gypsum\text{-}water}$

Salinity effects on oxygen and hydrogen isotopes during mineral precipitation have been reported for many different isotope systems (Sofer and Gat, 1972; Horita et al., 1996; Saccocia et al., 1998; Hu and Clayton, 2003). Gázquez et al. (2017b) determined

experimentally that the salt effect on $\alpha^{18}O_{gypsum\text{-}water}$ is negligible for salinities (i.e. NaCl) below 150 g/L, but it becomes significant for greater salt concentrations. Moreover, it was found that $\alpha D_{gypsum\text{-}water}$ shows a linear relationship with salinity (0.00003 per g/L of NaCl) even at relatively low ionic concentrations, so a salt correction needs to be considered when dealing with gypsum formed from brines (e.g. Dead Sea, evaporated seawater, etc.).

We corrected our theoretical results by the salt effects determined by Gázquez et al. (2017b) at 20 °C (with different NaCl concentration ranging from 0 to 300 g/L) (Fig. 4). Salt effects are assumed here to be the same at different temperatures. $\alpha^{18}O_{gypsum\text{-}water}$ and $\alpha D_{gypsum\text{-}water}$ at different salinities and temperatures can be obtained by using the following equations:

$\alpha^{18}O_{gypsum\text{-}water\ (S)} = \alpha^{18}O_{gypsum\text{-}water\ (0)}$; for salinity ≤150 g/L NaCl

$\alpha^{18}O_{gypsum\text{-}water\ (S)} = \alpha^{18}O_{gypsum\text{-}water\ (0)} + 1*10^{-5}*S$; for salinity >150 g/L NaCl

$\alpha D_{gypsum\text{-}water\ (S)} = \alpha D_{gypsum\text{-}water\ (0)}$; for salinity < 30 g/L NaCl

$\alpha D_{gypsum\text{-}water\ (S)} = \alpha D_{gypsum\text{-}water\ (0)} + 3*10^{-5}*S$; for salinity ≤ 30 g/L NaCl

where $\alpha^{18}O_{gypsum\text{-}water\ (S)}$ and $\alpha D_{gypsum\text{-}water\ (S)}$ are the isotope fractionation factors between gypsum hydration water and free water at different salinities, $\alpha^{18}O_{gypsum\text{-}water\ (0)}$ and $\alpha D_{gypsum\text{-}water\ (0)}$ are the theoretical fractionation factors at a given temperature that can be calculated from Table 1, and S is salinity in g/L of NaCl. Note that these salinity effects may be different from non-NaCl brines as observed for vapor-liquid water system (Stewart and Friedman, 1975; Horita et al., 1993).

The dependence of the triple oxygen isotope system (θ) with salinity has not been tested experimentally; however, given that the activity ratios of $^{18}O/^{16}O$ and $^{17}O/^{16}O$ are both controlled by the cations in solution, θ should not be affected to a significant extent. Therefore, the $\alpha^{17}O_{gypsum\text{-}water\ (S)}$ for different salinities may be calculated from $\alpha^{18}O_{gypsum\text{-}water\ (S)}$ and θ at a given temperature.

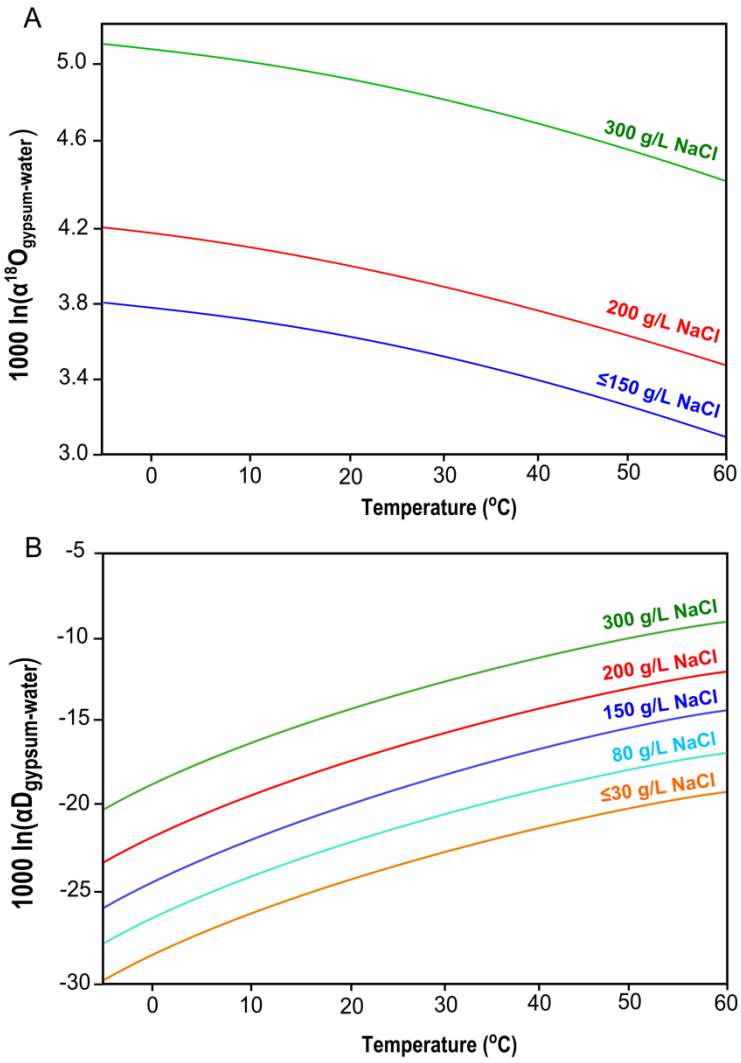

Fig. 4. 1000ln$\alpha^{18}O_{gypsum\text{-}water}$ (‰) (A) and 1000 ln$\alpha D_{gypsum\text{-}water}$ (‰) (B) of gypsum-water as a function of temperature at different NaCl concentrations.

5.4. On the opposite fractionations of D and ^{18}O in gypsum hydration water

Why is the $\alpha^{18}O_{gypsum\text{-}water} > 1$, whereas $\alpha D_{gypsum\text{-}water} < 1$? This observation sounds counterintuitive because if the vibrational modes for a chemical unit are stiffer in one system than in the other, the fractionation of all the species in that chemical unit should show the same trend. Although this effect has been known since the early 1960s (Gonfiantini and Fontes, 1963), no clear theoretical basis has been offered apart from some ad hoc explanations involving relationships between fractionation factor, bond length and cation/anion chemistry in aqueous solution (Oi Takao and Morimoto Hiroaki, 2013; Oi Takao et al., 2014). A general assumption has developed in the literature that the opposite fractionations may reflect the fact that the different species correspond to different chemical units. This is not the case, however, because both H and O are

replaced in the same hydration water molecule, and their respective fractionations are opposite. The correct explanation requires an examination of how different modes, with different participation in different species, become stiffer or softer when comparing two different systems. In this case, modes with a predominant H character in a water molecule may be stiffer in one of two systems, whereas modes with predominant O character are stiffer in the other one, albeit both being modes of the same molecule. This, of course, will be weighted by their relative participation in the partition functions, which we explore further below.

In order to explain this observation in more detail, we consider gamma phonons only for simplicity. Every possible single ^{18}O and D replacement site in gypsum hydration water is tested to ensure that inferences about the direction of isotopic fractionation ($\alpha^{18}O$ and αD) are consistent with the overall fractionation factor. In the isolated H_2O, there are three vibrational modes at 1590 cm^{-1}, 3661 cm^{-1} and 3778 cm^{-1}, which decrease to 1583 cm^{-1}, 3653 cm^{-1} and 3762 cm^{-1} respectively when ^{16}O is replaced with ^{18}O. The difference in frequency of each mode is very small, with the greatest difference being only 15 cm^{-1} for the highest frequency, the symmetric stretching. For gypsum, the O-H stretching at 3500 cm^{-1} is softer than the O-H stretching mode at 3653 cm^{-1} of the mother water, and it decreases by 70-90 cm^{-1} when replacing ^{16}O with ^{18}O. Thus, the frequency shift with heavy oxygen isotopic substitution is greater for the hydration water (70-90 cm^{-1}) than for the mother water (15 cm^{-1}). Equation 5 describes an exponential relation between the partition function (Q) and frequency (ω). The reduced fractionation factor $\beta^{18}O_{gypsum}$, with a larger $Q^{18}O/Q^{16}O$ ratio, will be greater than $\beta^{18}O_{water}$, with a smaller $Q^{18}O/Q^{16}O$ ratio; thus, $\alpha^{18}O$ (as described in eq. 3) will always be greater than 1.0.

Considering $\alpha D_{gypsum\text{-}water} < 1$, a similar explanation can be used for $\alpha^{18}O_{gypsum\text{-}water} > 1$ but it is complicated by the fact that the two hydrogen atoms in the hydration water contribute to the partition function differently because of their different orientations, which means they need to be considered separately. The three vibrational modes of H_2O, 1590 cm^{-1}, 3661 cm^{-1} and 3778 cm^{-1}, now decrease to 1394 cm^{-1}, 2700 cm^{-1}, and 3722 cm^{-1}, with differences of 196, 960 and 56 cm^{-1}, respectively, when H is replaced by D. These substitutions are much greater than the differences caused by the substitution of ^{16}O with ^{18}O, which is expected given the relative mass differences. For gypsum, there are two different configurations depending on the orientation of the hydrogen in the molecule with respect to the matrix of the host. (1) One of the two hydrogens in the hydration water molecule connects to an oxygen in a SO_4^{2-} group in the same layer by weak hydrogen bonding. (2) The second hydrogen atom connects to a SO_4^{2-} group oxygen in the next layer.

In the first case (1), there are only two vibrational frequencies that change significantly when replacing H with D: the mode at 1585 cm^{-1} shifts by 162 cm^{-1} to 1423 cm^{-1}, and the mode at 3264 cm^{-1} shifts by 876 cm^{-1} to 2388 cm^{-1}. The two frequency shifts of the H_2O

molecule (196 cm^{-1} and 960 cm^{-1}) are larger than those of gypsum hydration water (162 cm^{-1} and 876 cm^{-1}), which means the partition function ratio of D/H of the water molecule is larger than that of gypsum hydration water. This implies that the reduced fractionation factor $\beta^{18}O$ of gypsum hydration water is smaller than that of mother water. As a result, $\alpha D_{gypsum\text{-}water}$ will be less than 1.

In the second case (2), there are three vibrational frequencies that shift significantly when replacing H with D. The mode at 1585 cm^{-1} blue-shifts by 143 cm^{-1} to 1442 cm^{-1}, the mode at 3264 cm^{-1} blue-shifts by 805 cm^{-1} to 2459 cm^{-1}, and the mode at 3356 cm^{-1} blue-shifts by 74 cm^{-1} to 3282 cm^{-1}. For the first two vibrations, the frequency shift for the water molecule is still greater than that of gypsum by 53 and 155 cm^{-1}. In contrast, the third mode shift of H_2O is less than that of gypsum by 18 cm^{-1}. This is a much smaller difference than for the other two modes; thus, its effect on the partition function is minimal when the other two are taken into account. By considering the effect of these two different kinds of shifts on the partition function, we conclude that the partition function ratio of D/H of water is greater than that of gypsum for the second H position, which is similar to the case for the other hydrogen discussed previously. As a result, regardless of which hydrogen is considered, the conclusion that $\alpha D_{gypsum\text{-}water}$ is less than 1 will be the same.

6. Conclusion

We carried out first-principles calculations of oxygen and hydrogen isotopic fractionation factors between free water and the hydration water of gypsum and bassanite. Our theoretical fractionation factors, $\alpha^{18}O_{gypsum\text{-}water}$ and $\alpha D_{gypsum\text{-}water}$, agree well with experimental values. The temperature dependence of $\alpha^{18}O_{gypsum\text{-}water}$ is insignificant for most paleoclimate applications using gypsum hydration water, but the dependence of $\alpha D_{gypsum\text{-}water}$ on temperature is significant. For hydrogen isotopes, the formation temperature must be considered in order to ensure accurate fractionation factors are used, especially for hydrothermal or cryogenic gypsum deposits. The $\alpha^{18}O_{gypsum\text{-}water}$ and $\alpha D_{gypsum\text{-}water}$ at 0 °C are predicted to be 1.0038 and 0.9740, respectively.

The predicted $\alpha D_{gypsum\text{-}water}$ values at temperatures below 25 ^{o}C are consistently lower than the experimental observations. This can be explained by kinetic effects affecting $\alpha D_{gypsum\text{-}water}$ at lower temperatures because of fast gypsum precipitation under laboratory conditions. The triple oxygen isotope parameter ($\theta_{gypsum\text{-}water}$) is 0.52741±0.00063 in the temperature range of 0 to 60 °C, which roughly agrees with previous experimental results. This theoretical $\theta_{gypsum\text{-}water}$ value is probably more accurate than that derived by empirical results. We also explain why $\alpha^{18}O_{gypsum\text{-}water} > 1$ and $\alpha D_{gypsum\text{-}water} < 1$ from first-principles harmonic analysis, without resorting to an explanation involving different species being associated with different water sites in the mineral structure.

We calculate fractionation factors between free water and hydration water in basanite for

the first time. The $\alpha^{18}O_{bassanite\text{-}water}$ is similar to $\alpha^{18}O_{gypsum\text{-}water}$ in the 0 °C to 60 °C temperature range, whereas $\alpha D_{bassanite\text{-}water}$ is 0.009 to 0.02 lower than $\alpha D_{gypsum\text{-}water}$ in the same temperature range.

Acknowledgments

This research was supported by the ERC WIHM Project [#339694] to DAH. Computing support from Darwin HPC in the University of Cambridge, the TCM group cluster in the Physics Department of the University of Cambridge, and HPC in CIC Nanogune in San Sebastian, Spain, is gratefully acknowledged. Constructive comments and advice from Professor Edwin Schauble and three anonymous reviewers are warmly acknowledged.

References

Bao H., Cao X. and Hayles J. A. (2016) Triple oxygen isotopes: fundamental relationships and applications. *Annu. Rev. Earth Planet. Sci.* **44**, 463–492.

Barkan E. and Luz B. (2005) High precision measurements of 17O/16O and 18O/16O ratios in H2O. *Rapid Commun. Mass Spectrom.* **19**, 3737–3742.

Bezou C., Christensen A. N., Cox D., Lehmann M. and Nonat A. (1991) Structures cristallines de CaSO[4], 0,5H[2]O et CaSO[4], 0,6H[2]O. *Comptes Rendus Acad. Sci. Paris* **312**, 43–48.

Cao X. and Liu Y. (2011) Equilibrium mass-dependent fractionation relationships for triple oxygen isotopes. *Geochim. Cosmochim. Acta* **75**, 7435–7445.

Chen F., Turchyn A. V., Kampman N., Hodell D., Gázquez F., Maskell A. and Bickle M. (2016) Isotopic analysis of sulfur cycling and gypsum vein formation in a natural CO2 reservoir. *Chem. Geol.* **436**, 72–83.

Császár A. G., Czakó G., Furtenbacher T., Tennyson J., Szalay V., Shirin S. V., Zobov N. F. and Polyansky O. L. (2005) On equilibrium structures of the water molecule. *J. Chem. Phys.* **122**, 214305.

Evans N. P., Turchyn A. V., Gázquez F., Bontognali T. R. R., Chapman H. J. and Hodell D. A. (2015) Coupled measurements of δ18O and δD of hydration water and salinity of fluid inclusions in gypsum from the Messinian Yesares Member, Sorbas Basin (SE Spain). *Earth Planet. Sci. Lett.* **430**, 499–510.

Fontes J. C. and Gonfiantini R. (1967) Fractionnement isotopique de l'hydrogène dans l'eau de cristallisation du gypse. *C R Acad Sci* **265**, 4–6.

Franchi I. A., Wright I. P., Sexton A. S. and Pillinger C. T. (1999) The oxygen-isotopic composition of Earth and Mars. *Meteorit. Planet. Sci.* **34**, 657–661.

Garofalo P. S., Fricker M. B., Günther D., Forti P., Mercuri A.-M., Loreti M. and Capaccioni B. (2010) Climatic control on the growth of gigantic gypsum crystals within hypogenic caves (Naica mine, Mexico)? *Earth Planet. Sci. Lett.* **289**, 560–569.

Gázquez F., Calaforra J. M., Evans N. P. and Hodell D. A. (2017a) Using stable isotopes (δ17O, δ18O and δD) of gypsum hydration water to ascertain the role of water condensation in the formation of subaerial gypsum speleothems. *Chem. Geol.* **452**, 34–46.

Gázquez F., Calaforra J. M., Forti P. and Badino G. (2016) The Caves of Naica: A decade of research [Las Cuevas de Naica: Una década de investigación]. *Boletin Geol. Min.* **127**, 147–163.

Gázquez F., Evans N. P. and Hodell D. A. (2017b) Precise and accurate isotope fractionation factors (α17O, α18O and αD) for water and CaSO4·2H2O (gypsum). *Geochim. Cosmochim. Acta* **198**, 259–270.

Gázquez F., Mather I., Rolfe J., Evans N. P., Herwartz D., Staubwasser M. and Hodell D. A. (2015) Simultaneous analysis of 17O/16O, 18O/16O and 2H/1H of gypsum hydration water by cavity ring-down laser spectroscopy. *Rapid Commun. Mass Spectrom.* **29**, 1997–2006.

Gázquez F., Morellón M., Bauska T., Herwartz D., Surma J., Moreno A., Staubwasser M., Valero-Garcés B., Delgado-Huertas A. and Hodell D. A. (2018) Triple oxygen and hydrogen isotopes of gypsum hydration water for quantitative paleo-humidity reconstruction. *Earth Planet. Sci. Lett.* **481**, 177–188.

Gonfiantini R. and Fontes J. C. (1963) Oxygen isotopic fractionation in the water of crystallization of gypsum. *Nature* **200**, 644–646.

Gonze X. and Lee C. (1997) Dynamical matrices, Born effective charges, dielectric permittivity tensors, and interatomic force constants from density-functional perturbation theory. *Phys. Rev. B* **55**, 10355–10368.

Grauel A.-L., Hodell D. A. and Bernasconi S. M. (2016) Quantitative estimates of tropical temperature change in lowland Central America during the last 42 ka. *Earth Planet. Sci. Lett.* **438**, 37–46.

Greenwood J. P., Itoh S., Sakamoto N. and Yurimoto H. (2009) Hydrogen Isotope Measurements of Gypsum and Jarosite in Martian Meteorite Roberts Massif 04262: Antarctic and Houstonian Weathering. In *Lunar and Planetary Science Conference* Lunar and Planetary Inst. Technical Report. p. 2528.

Herwartz D., Surma J., Voigt C., Assonov S. and Staubwasser M. (2017) Triple oxygen isotope systematics of structurally bonded water in gypsum. *Geochim. Cosmochim. Acta* **209**, 254–266.

Hodell D. A., Turchyn A. V., Wiseman C. J., Escobar J., Curtis J. H., Brenner M., Gilli A., Mueller A. D., Anselmetti F., Ariztegui D. and Brown E. T. (2012) Late Glacial temperature and precipitation changes in the lowland Neotropics by tandem measurement of δ18O in biogenic carbonate and gypsum hydration water. *Geochim. Cosmochim. Acta* **77**, 352–368.

Horita J., Cole D. R. and Fortier S. M. (1996) *Salt effects on isotope partitioning and their geochemical implications: An overview*., United States.

Horita J., Cole D. R. and Wesolowski D. J. (1993) The activity-composition relationship of oxygen and hydrogen isotopes in aqueous salt solutions: II. Vapor-liquid water equilibration of mixed salt solutions from 50 to 100°C and geochemical implications. *Geochim. Cosmochim. Acta* **57**, 4703–4711.

Horita J. and Wesolowski D. J. (1994) Liquid-vapor fractionation of oxygen and hydrogen isotopes of water from the freezing to the critical temperature. *Geochim. Cosmochim. Acta* **58**, 3425–3437.

Hu G. and Clayton R. N. (2003) Oxygen isotope salt effects at high pressure and high temperature and the calibration of oxygen isotope geothermometers. *Spec. Issue Dedic. Robert Clayton* **67**, 3227–3246.

Luz B. and Barkan E. (2010) Variations of 17O/16O and 18O/16O in meteoric waters. *Geochim. Cosmochim. Acta* **74**, 6276–6286.

Massé M., Bourgeois O., Le Mouélic S., Verpoorter C., Spiga A. and Le Deit L. (2012) Wide distribution and glacial origin of polar gypsum on Mars. *Earth Planet. Sci. Lett.* **317**–**318**, 44–55.

Matsuhisa Y., Goldsmith J. R. and Clayton R. N. (1978) Mechanisms of hydrothermal crystallization of quartz at 250°C and 15 kbar. *Geochim. Cosmochim. Acta* **42**, 173–182.

Matsuyaba O. and Sakai O. H. (1973) Oxygen and hydrogen isotopic study on the water of crystallization of gypsum from the Kuroko type mineralization. *Geochem J* **7**, 153–165.

Méheut M., Lazzeri M., Balan E. and Mauri F. (2007) Equilibrium isotopic fractionation in the kaolinite, quartz, water system: Prediction from first-principles density-functional theory. *Geochim. Cosmochim. Acta* **71**, 3170–3181.

Méheut M. and Schauble E. A. (2014) Silicon isotope fractionation in silicate minerals: Insights from first-principles models of phyllosilicates, albite and pyrope. *Geochim. Cosmochim. Acta* **134**, 137–154.

Momma K. and Izumi F. (2011) ıt VESTA3 for three-dimensional visualization of crystal, volumetric and morphology data. *J. Appl. Crystallogr.* **44**, 1272–1276.

Natalicchio M., Dela Pierre F., Lugli S., Lowenstein T. K., Feiner S. J., Ferrando S., Manzi V., Roveri M. and Clari P. (2014) Did Late Miocene (Messinian) gypsum precipitate from evaporated marine brines? Insights from the Piedmont Basin (Italy). *Geology* **42**, 179–182.

Oi Takao and Morimoto Hiroaki (2013) Oxygen and Hydrogen Isotopic Preference in Hydration Spheres of Chloride and Sulfate Ions. *Z. Für Phys. Chem.* **227**, 807.

Oi Takao, Sato Kunihiko and Umemoto Kazuki (2014) Oxygen and Hydrogen Isotopic Preference in Hydration Spheres of Magnesium and Calcium Ions. *Z. Für Naturforschung A* **68**, 362.

Oroya J., Martin A., Callejo M., Marchesin F. and Garcia-Mota M. (2016) Numerical Atomic Orbitals Basis Dataset. Simune Atomistics Ltd. (www.simune.eu).

Perdew J. P., Burke K. and Ernzerhof M. (1996) Generalized Gradient Approximation Made Simple. *Phys Rev Lett* **77**, 3865–3868.

Perdew J. P., Ruzsinszky A., Csonka G. I., Vydrov O. A., Scuseria G. E., Constantin L. A., Zhou X. and Burke K. (2008) Restoring the Density-Gradient Expansion for Exchange in Solids and Surfaces. *Phys Rev Lett* **100**, 136406.

Perdew J. P. and Zunger A. (1981) Self-interaction correction to density-functional approximations for many-electron systems. *Phys. Rev. B* **23**, 5048–5079.

Prieto-Taboada N., Gómez-Laserna O., Martínez-Arkarazo I., Olazabal M. Á. and Madariaga J. M. (2014) Raman Spectra of the Different Phases in the CaSO4–H2O System. *Anal. Chem.* **86**, 10131–10137.

Qin T., Wu F., Wu Z. and Huang F. (2016) First-principles calculations of equilibrium fractionation of O and Si isotopes in quartz, albite, anorthite, and zircon. *Contrib. Mineral. Petrol.* **171**, 91.

Reynard B. and Caracas R. (2009) D/H isotopic fractionation between brucite Mg(OH)2 and water from first-principles vibrational modeling. *Chem. Geol.* **262**, 159–168.

Richet P., Bottinga Y. and Javoy M. (1977) A Review of Hydrogen, Carbon, Nitrogen, Oxygen, Sulphur, and Chlorine Stable Isotope Fractionation Among Gaseous Molecules. *Annu. Rev. Earth Planet. Sci.* **5**, 65–110.

Saccocia P. J., Seewald J. S. and Shanks W. C. (1998) Hydrogen and Oxygen Isotope Fractionation Between Brucite and Aqueous NaCl Solutions from 250 to 450°C. *Geochim. Cosmochim. Acta* **62**, 485–492.

Schauble E. A. (2004) Applying Stable Isotope Fractionation Theory to New Systems. *Rev. Mineral. Geochem.* **55**, 65.

Schoenemann S. W., Schauer A. J. and Steig E. J. (2013) Measurement of SLAP2 and GISP δ17O and proposed VSMOW-SLAP normalization for δ17O and 17Oexcess. *Rapid Commun. Mass Spectrom.* **27**, 582–590.

Schofield P. F., Knight K. S. and Stretton I. C. (1996) Thermal expansion of gypsum investigated by neutron powder diffraction. *Am. Mineral.* **81**, 847.

Showstack R. (2011) Mars Opportunity rover finds gypsum veins. *Eos Trans. Am. Geophys. Union* **92**, 479–479.

Sofer Z. (1978) Isotopic composition of hydration water in gypsum. *Geochim. Cosmochim. Acta* **42**, 1141–1149.

Sofer Z. and Gat J. R. (1972) Activities and concentrations of oxygen-18 in concentrated aqueous salt solutions: Analytical and geophysical implications. *Earth Planet. Sci. Lett.* **15**, 232–238.

Soler J. M., Artacho E., Gale J. D., García A., Junquera J., Ordejón P. and Daniel Sánchez-Portal (2002) The SIESTA method for ab initio order- N materials simulation. *J. Phys. Condens. Matter* **14**, 2745.

Steig E. J., Gkinis V., Schauer A. J., Schoenemann S. W., Samek K., Hoffnagle J., Dennis K. J. and Tan S. M. (2014) Calibrated high-precision $^{17\$}$O-excess measurements using cavity ring-down spectroscopy with laser-current-tuned cavity resonance. *Atmospheric Meas. Tech.* **7**, 2421–2435.

Stewart K. M. and Friedman I. (1975) Deuterium fractionation between aqueous salt solutions and water vapor. *J. Geophys. Res.* **80**, 3812–3818.

Tan H.-B., Huang J.-Z., Zhang W.-J., Liu X.-Q., Zhang Y.-F., Kong N. and Zhang Q. (2014) Fractionation of hydrogen and oxygen isotopes of gypsum hydration water and assessment of its geochemical indications. *Aust. J. Earth Sci.* **61**, 793–801.

Tritschler U., Kellermeier M., Debus C., Kempter A. and Colfen H. (2015a) A simple strategy for the synthesis of well-defined bassanite nanorods. *CrystEngComm* **17**, 3772–3776.

Tritschler U., Van Driessche A. E. S., Kempter A., Kellermeier M. and Cölfen H. (2015b) Controlling the Selective Formation of Calcium Sulfate Polymorphs at Room Temperature. *Angew. Chem. Int. Ed.* **54**, 4083–4086.

Troullier N. and Martins J. L. (1991a) Efficient pseudopotentials for plane-wave calculations. *Phys. Rev. B* **43**, 1993–2006.

Troullier N. and Martins J. L. (1991b) Efficient pseudopotentials for plane-wave calculations. II. Operators for fast iterative diagonalization. *Phys. Rev. B* **43**, 8861–8869.

Van Driessche A. E. S., Benning L. G., Rodriguez-Blanco J. D., Ossorio M., Bots P. and García-Ruiz J. M. (2012) The Role and Implications of Bassanite as a Stable Precursor Phase to Gypsum Precipitation. *Science* **336**, 69.

Wang Y.-W. and Meldrum F. C. (2012) Additives stabilize calcium sulfate hemihydrate (bassanite) in solution. *J Mater Chem* **22**, 22055–22062.

Wray J. J., Squyres S. W., Roach L. H., Bishop J. L., Mustard J. F. and Noe Dobrea E. Z. (2010) Identification of the Ca-sulfate bassanite in Mawrth Vallis, Mars. *Icarus* **209**, 416–421.

Zeebe R. E. (2010) A new value for the stable oxygen isotope fractionation between dissolved sulfate ion and water. *Geochim. Cosmochim. Acta* **74**, 818–828.